Numerical simulation of a piezoelectric loudspeaker including viscothermal effects for hearing aid applications

Gustavo C. Martins[a)]
Júlio A. Cordioli[b)]
Roberto Jordan[c)]
Department of Mechanical Engineering, Federal University of Santa Catarina
Campus Universitário, Florianópolis – SC Brazil, 88040-490.

Piezoelectric materials are already widely used in applications involving miniaturized components. The application of these materials in hearing aid receivers may present technical and economic advantages such as reducing the number of parts of the system and its manufacturing cost. The vibro-acoustic analysis of a piezoelectric component involves the construction of multi-physical models. Analytical models of piezoelectric components can be found in the literature, but these models involve in general very simple geometries or are very simplified. This work presents a multi-physical numerical model of a miniaturized speaker prototype. The numerical model was constructed using the Finite Element Method (FEM). This speaker is composed of a piezoelectric diaphragm coupled to a small cavity. The multi-physical model is composed of piezoelectric, structural and acoustic coupled FEM model. The acoustic model of the small cavity also accounts for thermal and viscous effects on the acoustic propagation. Finally, the multi-physical model is experimentally validated.

1 INTRODUCTION

The loudspeakers of current hearing aids are made up of electromagnetic, mechanical and acoustical components. The electromagnetic component is usually a complex system involving many parts that are assembled with great precision. The replacement of the electromagnetic component by a piezoelectric component can be advantageous, since the piezoelectric components usually need much fewer parts to fulfill the function of the electromagnetic components. Therefore, the application of piezoelectric components in loudspeakers for hearing aids can bring both technical (durability, consumption, etc) and economic advantages.

The modeling of miniaturized piezoelectric transducers, like loudspeakers and microphones for hearing aids, involves multi-physical models with strong coupling between the involved

a) email: gustavo.martins@lva.ufsc.br
b) email: cordioli@emc.ufsc.br
c) email: jordan@emc.ufsc.br

physics. In the literature, some analytical models of these components can be found[1-4]. However, these analytical models usually involve very simple geometries or are very simplified. These characteristics restrict the use of such models as a design tool for miniaturized piezoelectric transducers.

The aim of this paper is to develop and validate a numerical multi-physical model of a piezoelectric loudspeaker prototype so that it can be used as a design tool to analyze miniaturized piezoelectric loudspeakers for hearing aids. Simple loudspeaker prototypes were built , where the simple geometry was adopt to facilitate their manufacture. The loudspeaker prototypes were evaluated experimentally and the results used to validate the numerical models.

The numerical multi-physical model was implemented by using the Finite Element Method (FEM) using the commercial software COMSOL[5] together with lumped models. Two different geometries for the loudspeaker prototypes were tested and modeled. Each prototype was composed of a cylindrical cavity coupled to a piezoelectric diaphragm with the main differences in the diaphragm diameter and the cavity depth. One of the prototypes had a cavity with reduced deph so that the thermal and viscous effects could be investigated. As small cavities are found in hearing aid loudspeakers, these effects usually cannot be neglected in the acoustic propagation and they will be included also in the FEM acoustic model.

The paper starts with a presentation of the piezoelectric loudspeaker prototypes studied while the measuring system used is described. The multi-physical models built is described in Section 4. Finally, the results of the models and the experimental data are compared in section 5, followed by a comparison of the prototypes with commercial hearing aid loudspeakers and a sensitivity analysis.

2 THE PIEZOELECTRIC LOUDSPEAKER PROTOTYPES

The piezoelectric loudspeaker prototypes has a circular piezoelectric diaphragm consisting of a piezoelectric layer on a metal substrate, as shown in Fig. 1. This type of piezoelectric device is commercially available and used as a buzzer in different application. The metal substrate is made of brass, while the piezoelectric layer is comprised of PZT – 5A. The piezoelectric diaphragm is coupled to a cavity by using the fixing ring and the screws shown in Fig 1 (a). The piezoelectric diaphragm operates by applying an electric potential between the electrode above the piezoelectric layer and the metal substrate. The electric potential is applied by wired terminals like that shown in Fig. 1 (b).

Fig. 1(a) also shows a microphone coupler which is used to take measures of the sound pressure level (SPL) generated within the cavity through a side hole. The dimensions of the piezoelectric diaphragm and the microphone coupler are showed in Fig. 2 and Table 1.

The loudspeaker prototypes also included a cavity which was coupled to the piezoelectric diaphragm. The internal dimensions of these cavities are showed in the Fig. 3. The Prototype A has the cavity thickness below the diaphragm much larger than the Prototype B. This feature was chosen to verify the effects of thermal diffusion and viscous friction that occur in small cavities as reported in the literature[6].

3 EXPERIMENTAL SET-UP

The piezoelectric diaphragms were tested in two different conditions: in a free mechanical boundary condition and assembled with the loudspeaker cavity. The experimental setups used to perform the measurement for each condition are shown in Fig. 4. In the first setup, Fig. 4 (a), the frequency response function (FRF) measured with the Laser Vibrometer in relation to the AC

voltage applied to the wired terminals. In the second setup, Fig. 4 (b), a pressure/voltage FRF was measured using a 1/2" microphone connected to the coupler.

4 MULTI-PHYSICAL MODELS

To model the electro-vibro-acoustic behavior of the components shown in Fig. 1 (a), the piezoelectric, structural and acoustic models were considered. The piezoelectric diaphragm and the loudspeaker cavity were modeled using FEM models. The microphone coupler and its acoustic connection to the loudspeaker cavity were considered as acoustic tubes and were modeled using lumped models[7].

The multi-physical model domains are presented in Fig. 5. The coupling of these models was performed using transfer matrix by lumping the coupled FEM models as presented by Kampinga[7,8]. These models will be presented in the next sections.

4.1 Piezoelectric diaphragm FEM model

The piezoelectric diaphragm model was built through FEM formulation implemented in the commercial software COMSOL[5]. The piezoelectric component is modeled by the piezoelectric FEM formulation where the constitutive relation in Strain-Charge form is given by

$$\begin{aligned} \varepsilon &= s_E \sigma + d^T E \\ D &= d\sigma + \varepsilon_T E, \end{aligned} \tag{1}$$

where the meaning of these symbols is showed in Table 2.

The polarization direction of the piezoelectric material is the direction normal to the piezoelectric layer. The properties of the piezoelectric material were taken as equal to the PZT-5A. These properties are shown below:

$$s_E = \begin{bmatrix} 16.4 & -5.74 & -7.22 & 0 & 0 & 0 \\ -5.74 & 16.4 & -7.22 & 0 & 0 & 0 \\ -7.22 & -7.22 & 18.8 & 0 & 0 & 0 \\ 0 & 0 & 0 & 47.5 & 0 & 0 \\ 0 & 0 & 0 & 0 & 47.5 & 0 \\ 0 & 0 & 0 & 0 & 0 & 44.3 \end{bmatrix} \times 10^{-12} \ \frac{m^2}{N},$$

$$d = \begin{bmatrix} 0 & 0 & 0 & 0 & 584 & 0 \\ 0 & 0 & 0 & 584 & 0 & 0 \\ -171 & -171 & 347 & 0 & 0 & 0 \end{bmatrix} \times 10^{-12} \ \frac{C}{N},$$

$$\varepsilon_T = \begin{bmatrix} 1730 & 0 & 0 \\ 0 & 1730 & 0 \\ 0 & 0 & 1700 \end{bmatrix} \times 8.854e-12 \ \frac{F}{m}.$$

The metal substrate of the diaphragm was modeled with the standard structural FEM formulation. As specified by the manufacturer of the piezoelectric diaphragm, the metal substrate is made of brass. Since there was no information about the specific composition of this material, the material mechanical properties were slightly adjusted based on the average properties of brass alloys. These properties are shown in Table 3.

4.2 Loudspeaker cavity FEM model

Each loudspeaker cavity was modeled with different FEM formulation. The cavity of prototype A, as it has a larger thickness, was modeled using the standard acoustic FEM formulation. As

mentioned before, the cavity of prototype B is very thin and the thermal and viscous effects become more significant in the acoustic propagation. Therefore, an acoustic FEM formulation including these effects has been applied. This formulation is the same presented by Kampinga[7,8] and already implemented in COMSOL[5].

Air was considered as the fluid inside the cavities of the models. The properties of the air in the acoustic models are presented in the Table 4.

4.3 Microphone coupler lumped model

The microphone coupler and its acoustic connection to the loudspeaker cavity were considered as three coupled acoustic tubes as showed in Fig. 5. The transfer matrix for each tube can be obtained from the analytic solutions of the acoustic model resulting in

$$A_{tube} = \begin{bmatrix} \cos(kL) & -\frac{Z}{iS}\sin(kL) \\ \frac{iS}{Z}\sin(kL) & \cos(kL) \end{bmatrix}, \quad (2)$$

where L is the length of the tube, S is the surface area of the tube cross section, k is the wave number and Z is the characteristic impedance.

Tubes 2 and 3 also have small dimensions, and viscous and thermal were taken in account by using the Low Reduced Frequency (LRF) formulation. The LRF wave number and characteristic impedance depend on the tube cross section radius, the frequency and the air parameters. The parameters to set the LRF wave number and characteristic impedance for tubes is presented in[9]. The microphone coupler transfer matrix is then given by

$$A_{coupler} = A_{tube1}A_{tube2}A_{tube3}. \quad (3)$$

5 NUMERICAL AND EXPERIMENTAL RESULTS

5.1 Piezoelectric diaphragm in free mechanical boundary condition

Before analyze the complete loudspeaker model, the vibration behavior of the piezoelectric diaphragm was analyzed. The piezoelectric diaphragm was measured when placed on a foam to simulate a free mechanical boundary condition. Two samples of the diaphragm A and three samples of the diaphragm B were measured.

The piezoelectric diaphragm FEM model was built using the PZT-5A and Brass properties and applying the free mechanical boundary condition. A unit harmonic electric potential was applied at the position of the electrode above the piezoelectric component and the ground was applied at interface of piezoelectric and the metallic substrate. The velocity at the center of the diaphragms was calculated by the FEM model and the results were compared with the experimental data, as presented in Fig. 6.

As can be seen in Fig. 6, the FEM model showed good agreement with the measured data. The main differences observed between the model and experimental data are due to non-radial modes which were not excited in the FEM model since the excitation was symmetric. In the physical components, the presence of the electrodes and the wires, as well as geometric and material uncertainties are responsible for breaking the symmetry of the system and exciting non-radial modes. This can be seen in the Fig. 6 (a) in frequency around 12kHz and in the Fig. 6 (b) around 10kHz.

5.2 Prototypes coupled to the microphone

Following the validation of the FEM model of the piezoelectric diaphragm, the next step was the construction of the model of the diaphragm coupled to the cavity of the loudspeaker. A three-dimensional FEM coupled model was constructed for the Prototype A (named as Model A) . In this model, the diaphragm was clamped at the diameter of the loudspeaker cavity, as shown in Fig. 7 (a).

In Prototype B model (named as Model B), the visco-thermal acoustic FEM formulation was used for the cavity. Since the visco-thermal acoustic FEM model requires greater computational effort, a two-dimensional axisymmetric FEM model was used as presented in Fig. 7 (b).

Each model shown in Fig. 7 was used to obtain a transfer matrix A_{FEM} and a model of the whole system (including the tubes, coupler and microphones) was obtained by means of

$$\begin{Bmatrix} p \\ v \end{Bmatrix} = [A_{coupler}][A_{FEM}] \begin{Bmatrix} V \\ I \end{Bmatrix}, \tag{4}$$

where: p and v are the acoustic pressure and the velocity of volume at microphone membrane, respectively; V and I are the electric potential and the electric current at the electrode of piezoelectric diaphragm, respectively. By assuming a acoustic impedance to the microphone diaphragm[10], the acoustic pressure at the microphone can be calculated by applying a unit electric potential to the piezoelectric diaphragm.

Fig. 8 shows the comparison of the numerical results with the experimental data for the two models presented in the Fig. 7 coupled to the microphone coupler lumped model. The diaphragms were assembled and disassembled with the cavities at each measurement to verify the variability of the diaphragm assembly, as shown by the gray curves in the Fig. 8.

It can be noted in Fig. 7 that the diaphragm boundary condition appears to be more rigid than the actual condition of the experiment. This could be expected since the prototype structure is not sufficiently stiff to impose a clamped condition to the brass plate. One alternative to reduce the errors associated with the diaphragm boundary conditions is to considered a larger diameter than the actual one. As can be observed in Fig. 8, such adjustment results in SPL in the microphone very similar to the experimental data below 8 kHz. Similar results were obtained with prototype B.

5.3 Sensitivity Analysis

In this section, the sensitivity of some geometric parameters of prototype B are evaluated in order to improve its performance. Considering the Model B coupled to the microphone coupler and the clamped boundary condition applied at cavity diameter, the following parameters were evaluated: thickness of the metal substrate, thickness of the piezoelectric layer and the cavity and the diaphragm diameter together.

Fig. 9 shows the results of the SPL by varying the thickness of the metal substrate and the thickness of the piezoelectric layer, keeping other parameters constant. The results show that the reduction of the thickness could increase the SPL improving the performance of the loudspeaker.

Fig. 10 shows the results of the SPL when varying the diameter of the cavity and the diaphragm together, keeping other parameters constant. These results shows that the reduction of the diameter could decrease the SPL of the loudspeaker. This was expected because the reduction of the diaphragm diameter decreases both its area and its flexibility, decreasing the sound radiation and its vibration response.

5.4 Comparison with commercial hearing aid loudspeakers

Fig. 11 shows the Sound Pressure Levels (SPL) obtained applying an unit electric potential at the terminals of the three commercial hearing aid loudspeakers and the prototypes analyzed at this paper. It can be seen that the commercial loudspeakers produce higher SPL for the same voltage for most of the frequency range, especially at low frequencies. However, prototype B displays similar or higher SPL than commercial loudspeakers for frequencies above 6 kHz. It may be noted as well that prototype B has a better performance than the prototype A, presenting an indicative to improve the piezoelectric loudspeaker design.

Fig. 12 shows a comparison of the SPL for current Model B and a proposed geometry for a piezoelectric hearing aid loudspeaker. This proposed geometry has 0.02 mm of thickness for the piezoelectric layer and the metal substrate and has 3 mm of diameter for the diaphragm and the cavity together. The other geometric parameters are the same as current geometry. This comparison shows that the effect of diaphragm diameter reduction dominates the thickness reduction effects, resulting in a decrease of the performance of this system. Therefore, other parameters of the system need to be adjusted if a similar performance to the commercial loudspeakers for hearing aids is to be obtained.

6 DISCUSSION AND CONCLUSIONS

This paper presented a multi-physical model to analyze piezoelectric loudspeaker prototypes. A piezoelectric diaphragm FEM model was built and experimentally validated. The FEM model of the piezoelectric diaphragm was then coupled to a standard acoustic FEM model (prototype A) and to a visco-thermal acoustic FEM model (prototype B) for the case of small cavities. The results were compared with the experimental data also showing good agreement between them, although it was necessary adjusting the diaphragm boundary condition. A initial comparison with commercial loudspeakers for hearing aids was performed, and it was observed that the geometries considered display lower SPL levels that the commercial loudspeakers. However, a sensitivity analysis has shown that the performance of the loudspeakers may be improved through a proper design of this geometry and material properties.

7 ACKNOWLEDGEMENTS

This research was supported by FINEP Foundation and AMPLIVOX Company, and we would like to thank them for their assistance.

8 REFERENCES

1. P. Lotton, M. Bruneau, Z. Skvor and A.M. Bruneau, “A model to describe the behavior of a laterally radiating piezoelectric loudspeaker”. *Applied Acoustics*, 58, (1999).
2. Q. Wang, S.T. Quek, C.T. Sun and X. Liu, “Analysis of piezoelectric coupled circular plate”. *Smart Mater. Struct*, 10, (2001).
3. C. Mo, R. Wright, W.S. Slaughter, W.W. Clark, “Behaviour of a unimorph circular piezoelectric actuator”. *Smart Mater. Struct*, Volume 15, (2006).
4. B. Gazengel, P. Hamery, P. Lotton, and A. Ritty, “A Dome Shaped PVDF Loudspeaker Model”. *Acta Acustica*, Volume 97, pp. 800-808, (2011).
5. *COMSOL Multiphysics user’s guide*, 4.2a edition, (2011).

6. W. R. Kampinga, C. Bossaart, Y. H. Wijnant, A. de Boer. "The coupling of a hearing aid loudspeaker membrane to visco-thermal air layers". *InProceedings of ICSV 14*. Cairns, Australia, (2007).
7. W.R. Kampinga; *Viscothermal acoustics using finite elements : analysis tools for engineers*, PhD Thesis, University of Twente, Enschede, (2010).
8. W.R. Kampinga; Y.H. Wijnant, A. de Boer, "Performance of several viscothermal acoustic finite elements". *Acta Acustica*, Volume 96, pp. 115-124, (2010).
9. H. Tijdeman. "On the propagation of sound waves in cylindrical tubes". *Journal of Sound and Vibration*, 39(1):1–33, (1975).
10. Brüel & Kjaer, *Technical Documentation: Microphone handbook Vol. 1: Theory*. Naerum, Denmark, (1996).

Table 1 – Dimensions (in millimeters) of the piezoelectric diaphragms.

Dimension	**Dm**	**Tm**	**Dp**	**Tp**
Diaphragm A	20	0.20	14	0.22
Diaphragm B	15	0.10	10	0.12

Table 2 – Symbol definitions for the constitutive relation in Strain-Charge form.

Symbol	**Units**	**Meaning**
$\boldsymbol{\sigma}$	N/m^2	stress component vector
$\boldsymbol{\varepsilon}$	m/m	strain component vector
$\boldsymbol{E}$	N/C	electric field component vector
$\boldsymbol{D}$	C/m^2	electric charge density displacement component vector
$\boldsymbol{s_E}$	m^2/N	compliance coefficient matrix
$\boldsymbol{\varepsilon_T}$	F/m	electric permittivity matrix
$\boldsymbol{d}$	C/N	piezoelectric coupling coefficient matrix

Table 3 – Brass mechanical properties.

Young's Modulus	110 [GPa]
Density	8000 [kg/m^3]
Poisson's Ratio	0.32
Loss Factor	0.025

Table 4 – Properties of the air in the acoustic models.

Equilibrium temperature	293 [K]
Equilibrium pressure	101325 [Pa]
Equilibrium density	1.201 [kg/m^3]
Sound velocity	344 [m/s]
Viscosity	1.81 E-5 [Pa.s]
Bulk viscosity	1.09 E-5 [Pa.s]
Thermal conductivity	0.0256 [W/(m.K)]
Heat capacity at constant pressure	1004 [J/(kg.K)]
Specific gas constant	288 [J/(kg.K)]

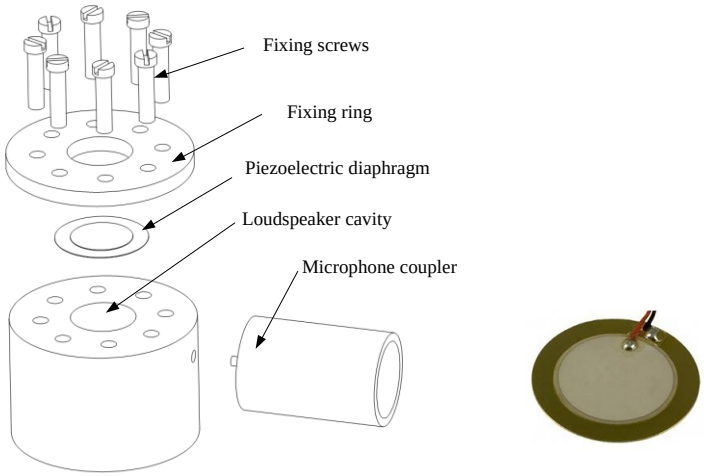

a) *b)*

Fig. 1 – Components of the piezoelectric loudspeaker prototype with the microphone coupler (a) and a picture of the piezoelectric diaphragm used (b).

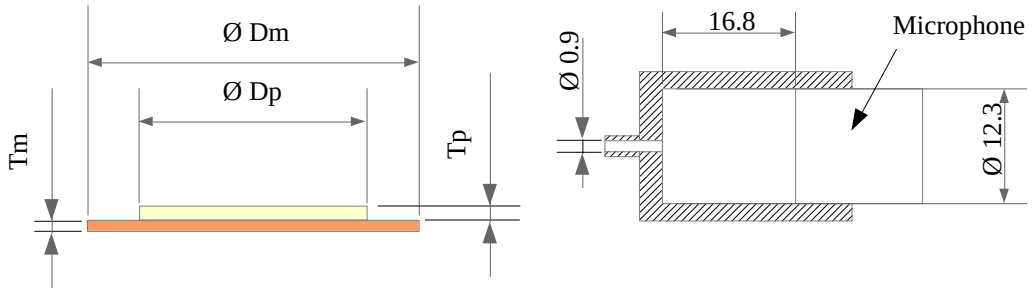

a) *b)*

Fig. 2 – Dimensions (in millimeters) of the piezoelectric diaphragm (a) and the microphone coupler (b).

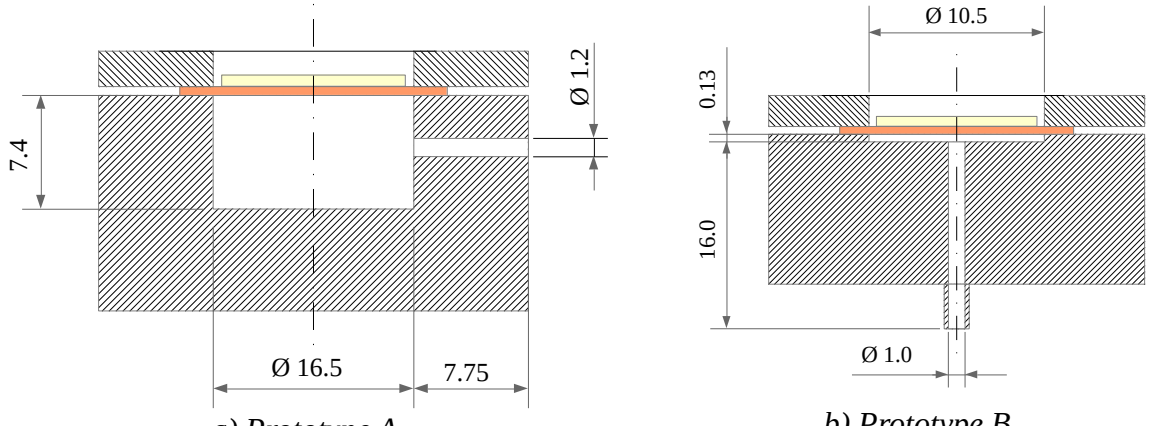

a) Prototype A *b) Prototype B*

Fig. 3 – Dimensions (in millimeters) of the prototype loudspeaker cavities.

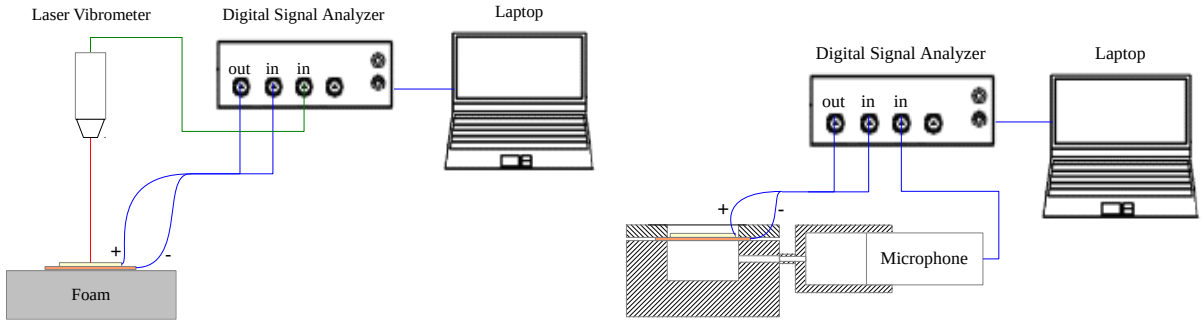

a) *b)*

Fig. 4 – Experimental setups to take the measurement of the diaphragms in a free mechanical boundary condition (a) and it assembled with the loudspeaker cavities (b).

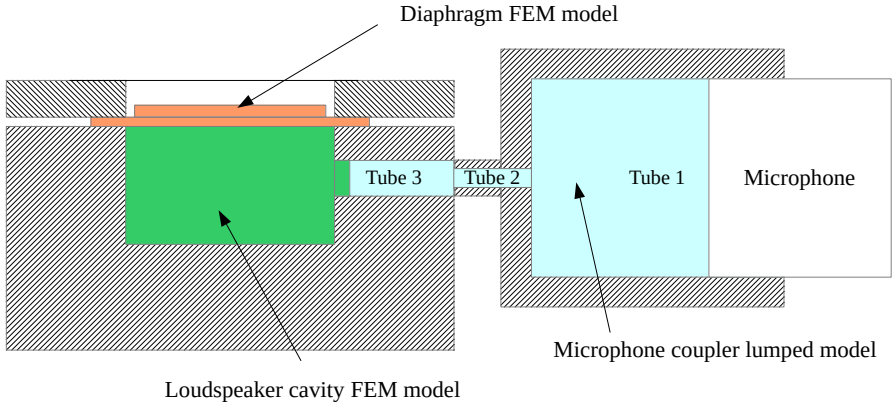

Fig.5 – Multi-physical model domains.

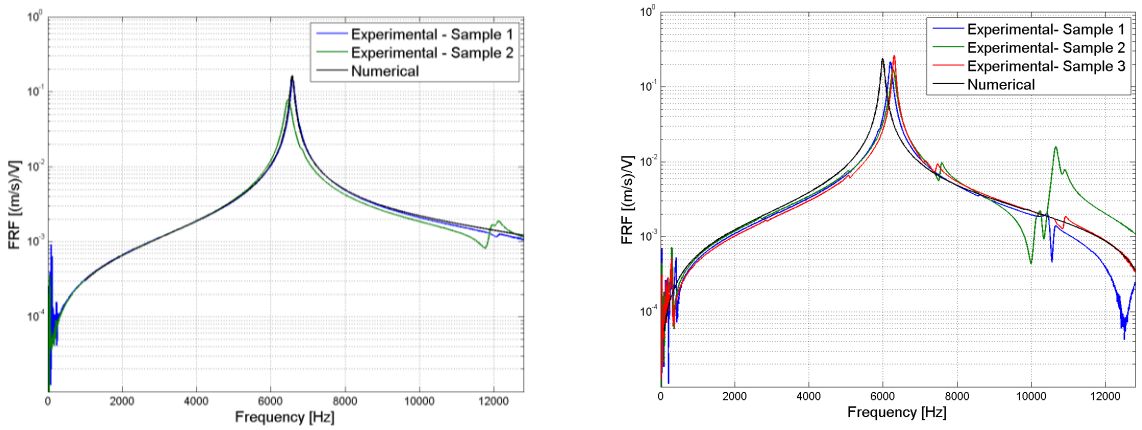

a) *b)*

Fig. 6 – Comparison of numerical approach and experimental data for diaphragm A (a) and diaphragm B (b) in free mechanical boundary condition.

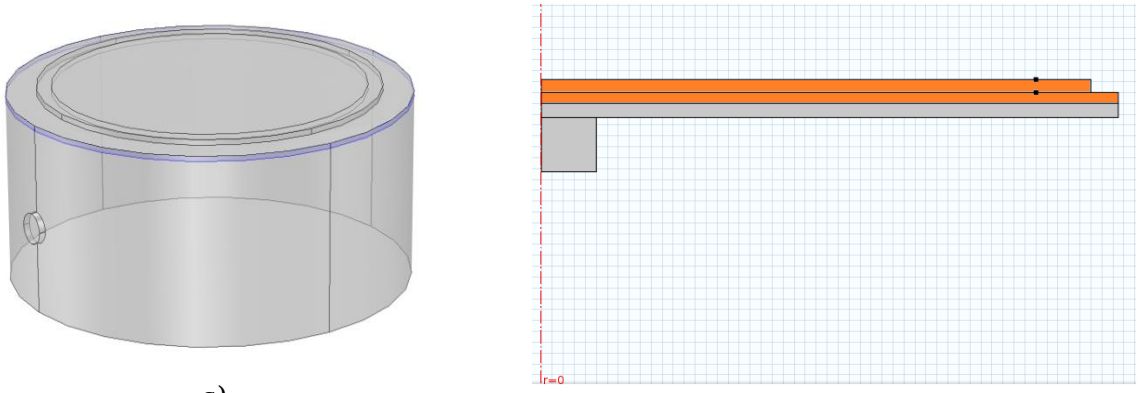

a) *b)*

Fig. 7 – Three-dimensional FEM model of Prototype A (a) and the two-dimensional FEM model of Prototype B (b).

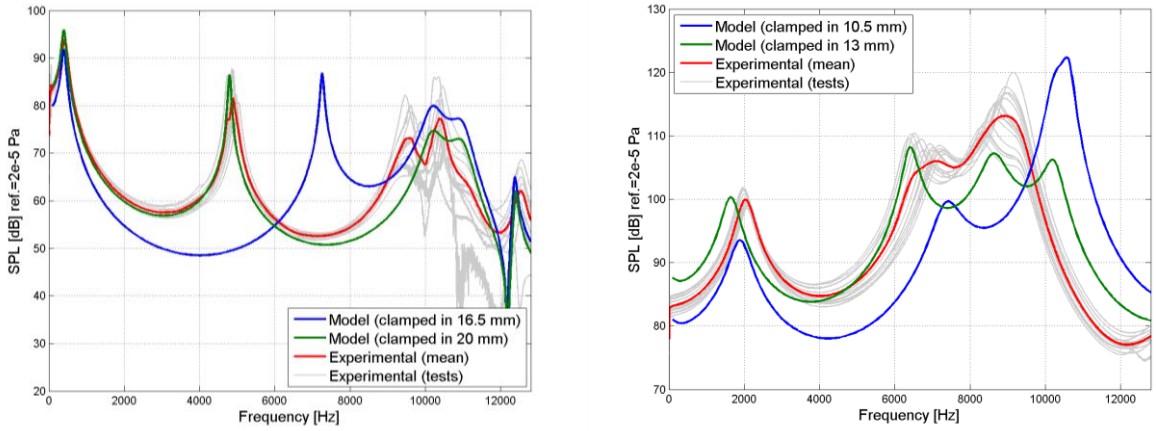

a) *b)*

Fig. 8 – Comparison of numerical approach and experimental data for the Model A (a) and the Model B (b) coupled with the microphone coupler (V=1Volt).

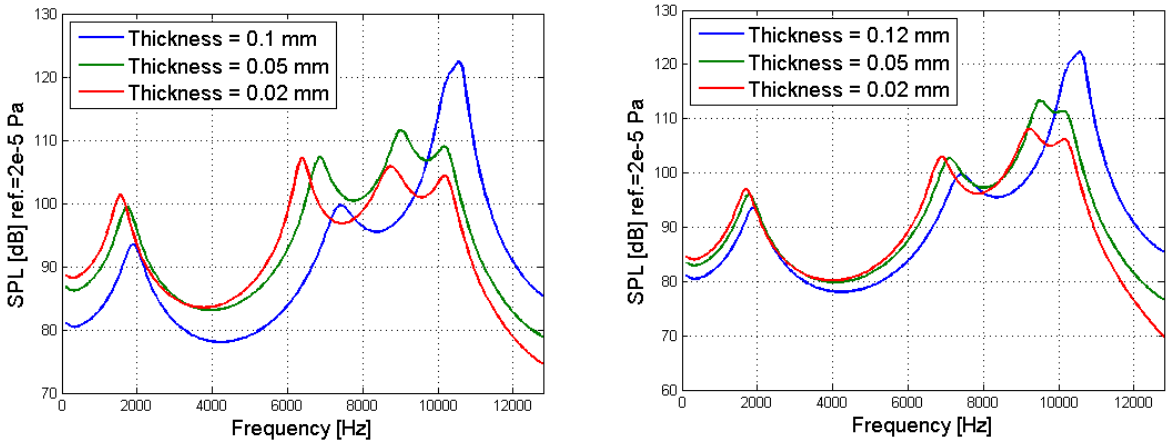

a) *b)*

Fig. 9 – SPL results for the variation of the metallic substrate thickness (a) and the piezoelectric layer thickness (b) (V=1Volt).

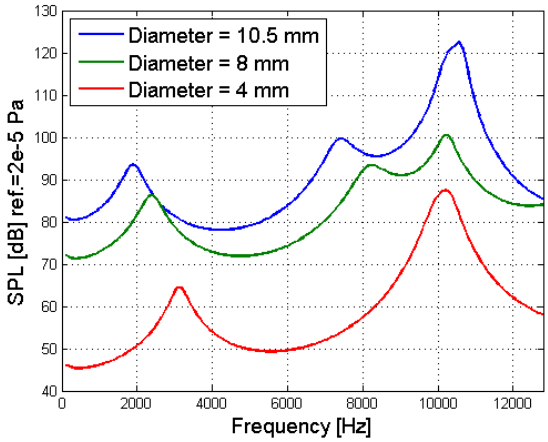

Fig. 10 – SPL results for the variation of the cavity and diaphragm diameter.

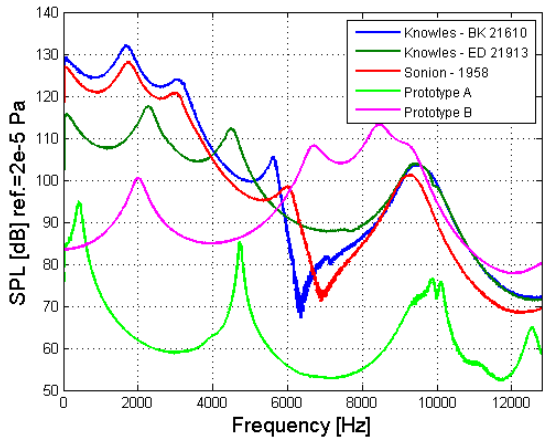

Fig. 11 – Comparison of Sound Pressure Level (SPL) of the commercial hearing aid loudspeakers and the piezoelectric loudspeaker prototypes ($V = 1Volt$).

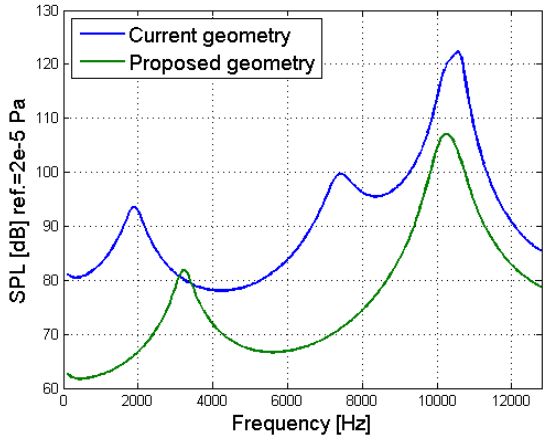

Fig. 12 – Comparison of the SPL for current Model B and a proposed geometry for a piezoelectric hearing aid loudspeaker ($V = 1Volt$).